Available online at www.sciencedirect.com
SCIENCE DIRECT®
ELSEVIER
Nuclear Instruments and Methods in Physics Research B 211 (2003) 453–459
NIM B
Beam Interactions with Materials & Atoms
www.elsevier.com/locate/nimb

# Stopping power of Au for silver ions at low velocities

R.V. Ribas [a,*], N.H. Medina [a], N. Added [a], J.R.B. Oliveira [a], E.W. Cybulska [a], M.N. Rao [a], W.A. Seale [a], F. Brandolini [b], M.A. Rizzutto [a], J.A. Alcántara-Núñez [a]

[a] *Departamento de Física Nuclear Instituto de Fisica, Universidade de São Paulo, CP 66318, 05314-970 Sao Paulo, SP Brazil*
[b] *Dipartimento di Fisica dell'Università and INFN, Sezione di Padova, Italy*

Received 13 May 2003

**Abstract**

Energy loss measurements for the slowing down of Ag ions in Au, in the velocity range $1.6v_0 < v < 4.4v_0$, where $v_0$ is the Bohr velocity, are presented. The measurements were performed using the Doppler shift technique and also with a new method, where a secondary beam of low velocity heavy ions is produced by elastic scattering of the accelerated beam. The results are compared to the SRIM2000 calculations (www.srim.org) and to recent measurements in this velocity region.


*PACS:* 34.50.Bw
*Keywords:* Stopping power; Energy loss

## 1. Introduction

The stopping power of solids for heavy ions at low velocities is still poorly known. Since ab initio calculations are unable to produce reliable quantitative estimates, most of the predictions in use are of a semiempirical nature. In the case of heavy ions, the large number of combinations of $Z_1$, $Z_2$, wide range of energies, and sparse experimental data, make even the semiempirical predictions contain, in general, large uncertainties. This is especially true at low velocities (around and below the Bragg peak) due to the additional difficulties in predicting the rapid changes in the charge state of the slowing ion, and to the complicated dependence of the stopping force on the atomic numbers. An accurate knowledge of the stopping force in this low velocity region is necessary in many experimental techniques, like those for ion implantation, surface analysis, etc. In nuclear physics, for instance, the measurement of pico-second lifetimes of nuclear states is normally performed with the Doppler shift attenuation method [1]. Here the knowledge of the stopping power as a function of the velocity of the recoiling excited nucleus is used to determine the timescale for the nucleus decaying in flight while slowing down in a heavy substrate, usually Au or Pb. Since the

* Corresponding author. Fax: +55-11-3814-0503.
*E-mail address:* ribas@if.usp.br (R.V. Ribas).

0168-583X/$ - see front matter 
doi:10.1016/S0168-583X(03)01519-2

velocities acquired by the nucleus come from the kinematics of a nuclear reaction induced by heavy ions, their initial values will be, in most cases, a few percent of the velocity of light. For this velocity region (i.e. $v < v_e = v_0 Z_1^{2/3}$, where $v_e$ is the Thomas–Fermi velocity of the electrons in an atom with atomic number $Z_1$ and $v_0 \simeq c/137$ is the Bohr velocity), one of the most commonly used semiempirical calculations is that developed by Ziegler, Biersack and Littmark (ZBL) [2,3]. In that work, both the energy losses by inelastic collision of the ion with electrons of the target (electronic stopping power) as well as the more sudden losses by atom-atom elastic collisions, which are important in this velocity region, are taken into account. In this paper, we present experimental data for the stopping of silver ions in gold at velocities below $4.4v_0$, using two different techniques. The results are compared with the predictions of the ZBL parameterization and with other recent measurements in the same velocity region.

## 2. Measurements and analysis

The experimental data we present here were obtained with two different techniques. In the first one the Doppler shift method, already employed in several other measurements [4–6], was used. In this technique, the mean energy of Coulomb excited target nuclei ($^{107,109}$Ag in the present case) after traversing the stopper foil, is measured by the determination of the Doppler shift in the energy of the $\gamma$ rays emitted by the decaying nuclear states. Excited nuclei were produced by collision with heavy projectiles ($^{16}$O, $^{28}$Si) and the nuclei recoiling in a cone centered around 0° were selected by imposing time coincidence between the projectiles scattered near 180°, detected in a Si annular detector, and the $\gamma$ rays.

For velocities below $\sim 2v_0$, the use of the Doppler shift technique would produce results with large uncertainties, due to the small difference between shifted and unshifted energies. In order to obtain reliable data for these energies, we developed a new technique which proved to be better than the one used for the preceding measurements. The second set of data was obtained using the secondary heavy ion beam (Ag in the present case) produced by elastic scattering of the primary accelerated beam ($^{16}$O, $^{28}$Si), the scattered particle being detected in kinematic coincidence with the recoil. Using a highly collimated geometry, it is possible to have a well defined secondary beam, both in energy and in direction.

### 2.1. Measurements with the Doppler shift method

The $\gamma$-ray energies were measured with a HP germanium detector placed at the 0° direction, with about 2.3 keV FWHM energy resolution for the $^{60}$Co lines. The stopper employed consisted of a rolled Au foil, of $2.02 \pm 0.04$ mg/cm$^2$ thickness, determined by measuring the energy loss of $\alpha$ particles from a $^{241}$Am source. The uniformity of the foil was measured in two perpendicular directions also using $\alpha$-particle energy loss. After the thickness determination, about 0.5 mg/cm$^2$ natural silver was evaporated onto one side of the foil. Before the measurements, the composite target was kept in vacuum or an argon atmosphere to avoid contamination or oxidation of the surfaces. A thick Ta foil with a thin natural Ag layer evaporated onto one side was used as a beam catcher, positioned near the $\gamma$-ray detector. This provided unshifted Ag $\gamma$-ray energies which, recorded simultaneously with the Doppler shifted lines were used as references to measure the energy shifts. The $\gamma$-ray lines from Coulomb excited levels on Au and Ta were also seen in the coincidence spectra as chance events and used for calibration of the energy scale. A typical $\gamma$-ray spectrum in coincidence with the backscattered beam particles is shown in Fig. 1. Most of the lines in this spectrum, including those from Ag stopped in Ta, are removed by subtracting the spectrum produced only by chance coincidences. In order to obtain the recoil energy from the $\gamma$-ray energy shifts, we must include a series of corrections due to the angular distribution of the scattered projectiles and of the $\gamma$ rays on the detector face, energy dependence of the efficiency of the $\gamma$-ray detector and the relativistic effects in the solid angles viewed from the source reference system. These corrections are described in detail in [7]. The average energy of the recoiling ions, before entering the stopper material, was

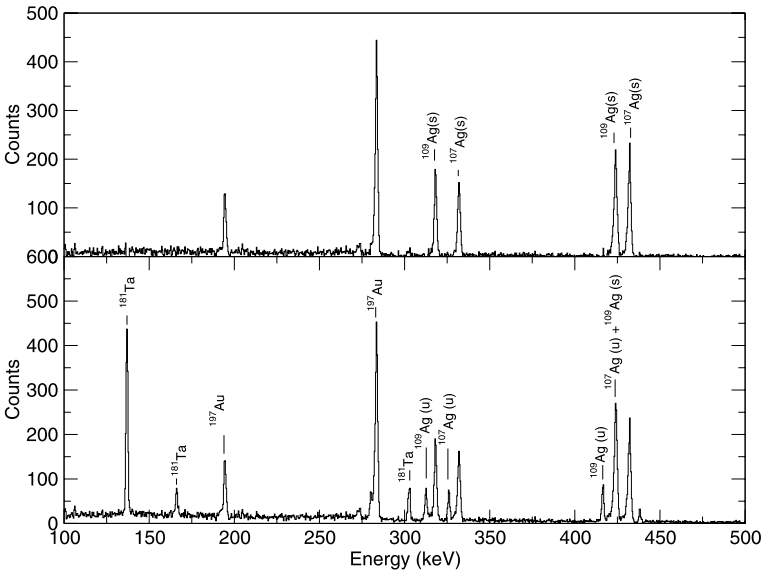


Fig. 1. γ-Ray spectrum showing shifted (s) and unshifted (u) peaks in coincidence with backscattered beam particles before (bottom) and after (top) chance subtraction, where only the lines from $^{107,109}$Ag and from $^{197}$Au remain.

determined by careful simulation of the processes involved, including the angular dependence of the Coulomb excitation process, solid angles and target thickness [6].

The experimental energy losses, obtained at four different initial Ag energies, are shown in Table 1. The uncertainties shown in the energy losses are mainly from the centroid determinations of the shifted and unshifted γ-ray peaks. As the relative uncertainties in the energy loss increase with the inverse of the energy difference between the shifted and unshifted peaks, a quite thick stopper foil had to be employed. In this way, a large fraction of the initial energy is lost in the stopper (about 50%) and the measured $\Delta E/\Delta x$ cannot be related to the stopping power at the average energy. The data analysis was carried out by using a reasonable parameterization for both the electronic ($S_e$) and the nuclear ($S_n$) stopping powers in the range of energy of the measurements and relating the experimental values of the stopper thickness $\Delta x$, the measured energy loss $\Delta E$ and the initial energy $E_i$ by the integral

$$\Delta x(E_i, \Delta E) = \int_{E_i}^{E_i - \Delta E} \frac{dE}{S_e(E) + S_n(E)}.$$

In a similar way, using the fitted $S_e$, $\Delta E_{fit}$ corresponding to the loss in the stopper can be obtained. Since, in the energy region of the measurements, the contribution of $S_n$ to the stop-

Table 1
Results from the measurements using the Doppler shift technique

| $E_i$ | $v/v_0$ | $\Delta E_{exp}$ | $\Delta E_{fit}$ | $\Delta E_{ZBL}$ |
|---|---|---|---|---|
| 35.1 | 3.62 | 17.3 (6) | 17.3 | 16.6 |
| 41.3 | 3.93 | 19.4 (5) | 19.8 | 18.6 |
| 46.3 | 4.16 | 21.6 (4) | 21.8 | 20.0 |
| 52.3 | 4.42 | 24.4 (6) | 24.0 | 21.6 |

All energies are in MeV. $E_i$ are the Ag initial energy and $v/v_0$ the corresponding velocity relative to $v_0$. $\Delta E_{exp}$ the measured energy loss in the Au foil. $\Delta E_{fit}$ and $\Delta E_{ZBL}$ are the energy losses obtained with the fitted and original ZBL [3] functions (see text). The energy losses were measured with a stopper foil 2.02 mg/cm$^2$ thick.

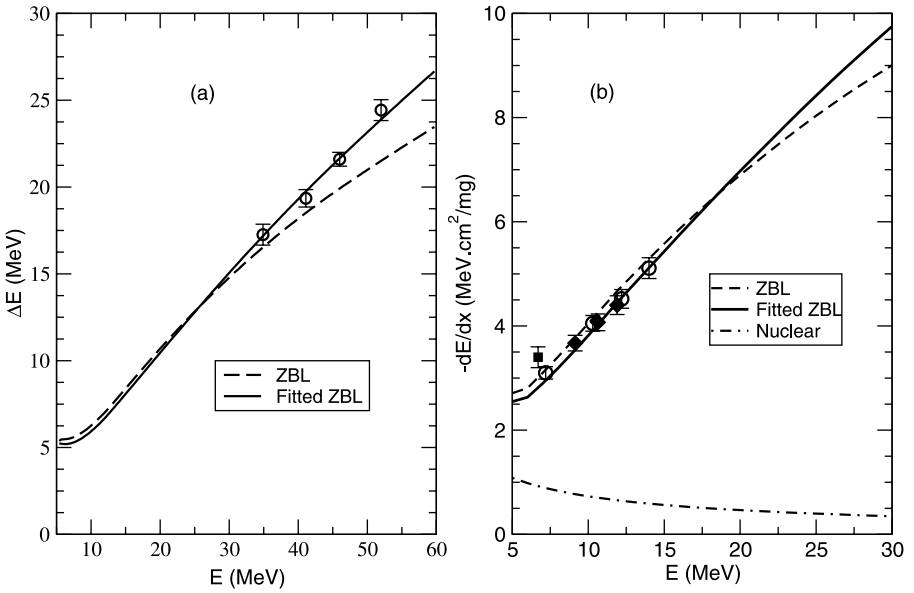


Fig. 2. (a) Energy loss in the Au target, measured with the Doppler shift method, as a function of the initial Ag energy. The solid curve corresponds to the fit of the ZBL parameterization to the experimental points; (b) circles and diamonds: data obtained with the elastic scattering technique, labeled Exp. I and Exp. II in Table 2, respectively. Square: datum from [4]. These data are compared to the fitted function (see text) and to the ZBL predictions [3].

ping is less than 5%, the predicted $S_n$ from [2] was used. For $S_e$, we adopted the same procedure used in [3], where the electronic stopping is obtained by scaling the stopping power of Au for protons with the effective charge of the Ag ions as a function of its velocity. We then introduced multiplying factors in three of the coefficients for the proton curve of these calculations, which were found to be the most influential in the energy region related to the present measurements. The actual function used for protons in [3] including the multipliers $F_1$, $F_2$ and $F_3$ is

$$S_e^{\mathrm{Low}}(E) = 1.041E^{0.00405} + F_1 \cdot 5.61E^{F_2 \cdot 0.439},$$

$$S_e^{\mathrm{High}}(E) = \frac{F_3 \cdot 3646}{E^{0.869}} \ln\left(\frac{2878}{E} + 0.0139E\right),$$

with

$$S_e = \frac{S_e^{\mathrm{Low}} S_e^{\mathrm{High}}}{S_e^{\mathrm{Low}} + S_e^{\mathrm{High}}}.$$

The best values for these multipliers were found in a least-square procedure for $\Delta x$ as a function of $(E_i, \Delta E)$ in the integral shown above: $F_1 = 0.87(3)$, $F_2 = 1.00(1)$, $F_3 = 1.46(8)$. In Fig. 2(a) we show the experimental values of the energy loss as a function of the initial energy of the Ag ions, and also the prediction of both the adjusted curve (solid line) and the original parameterization of [3] (dashed line). The predicted $\Delta E$s obtained with the coefficients from [3] are also shown in Table 1.

### 2.2. Measurements with the elastic scattering method

The experimental set up for the measurements using the elastic scattering technique is shown in Fig. 3. The Si detector for the scattered primary beam (Det1) was positioned at $\theta_{sc} = 60°$ with a total angular aperture of about 2°. For $^{16}O$ and $^{28}Si$ primary beams, the corresponding Ag recoil angle ($\theta_{rec}$) was about 55°. The stopper foil was placed in a mobile holder, and could be moved into or away from the secondary beam direction. The energy of the recoiling silver ions was also measured with a Si detector (Det2), with and

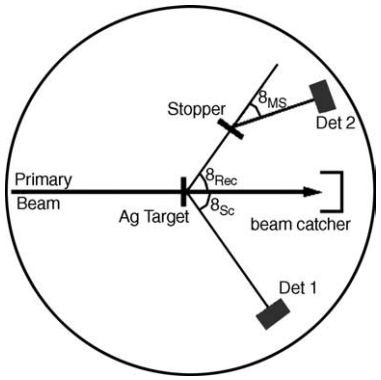


Fig. 3. Geometry employed for the elastic scattering technique. The angle $\theta_{sc}$ is fixed at 60° and $\theta_{rec}$ is taken from kinematics. $\theta_{ms}$ can be varied in order to measure the angular distribution after multiple scattering. For the energy-loss measurements, the $\theta_{ms} = 0$ can be precisely found by measuring the maximum of the distribution, without the stopper foil.

without the stopper foil intercepting the recoiling Ag ions. The relation of the converted pulse hight to the recoil energy was found to be linear in the region of the measurements, even if the effect of the detector's dead layer should play an important role for these low energy particles. For measurements in a larger energy range, non-linear calibration curves may be necessary. The correct kinematic angle for the secondary beam was found by experimentally determining the maximum of the angular distribution of the recoils, measured without the stopper foil.

In order to calibrate the energy scale of the recoils detector, the energies of the recoiling Ag ions were calculated using a Monte Carlo procedure: first, the scattering of the beam is sorted at a random angle (within the scattering detector solid angle) and position in the target. Then the energy loss of the beam up to that point, the recoil energy and angle of the Ag ions are calculated. Finally, the electronic energy loss and the Ag–Ag elastic collisions in the target are followed using the formalism described in [8]. In these calculations, the electronic stopping power and scattering function from [2] were used. With the target thickness usually employed ($\sim$80 μg/cm$^2$), these corrections were rather small and not critically dependent on the accuracy of the stopping power data used in the simulations. We also simulated the dependence of the energy of the Ag ions, after passing the stopper foil, as a function of the average multiple scattering angle (see Fig. 3). Since the detector for the recoils cover only a small fraction of the total angular distribution, the measured energy should be smaller than the average including all angles. The simulation has shown that this difference is less than 1% for the worst case (lower energy). A typical spectrum for the recoils detector is shown in Fig. 4. Since for the present case the scattering and recoil angles are almost identical, due to the angular spread of the recoils, the reverse solution (with the scattered primary beam coming to this detector and the recoil to the scattering detector) is also seen.

In the measurements using this method, the thickness of the Au stopper, $0.62 \pm 0.02$ mg/cm$^2$ is much smaller than that of the one employed with the Doppler shift technique. With the smaller stopping power for the lower energies used in the measurements, the energy losses in the stopper are now much smaller, so the differential approach $\left(\frac{\Delta E}{\Delta x} \simeq \frac{dE}{dx}(\overline{E})\right)$ could be used.

The results of the measurements of the stopping of Ag in Au using this technique are shown in Table 2. In Fig. 2(b), the experimental data are shown along with the predictions of the ZBL program, using both the original parameter set and also the adjusted parameters obtained for the measurements using the Doppler shift method, at higher energies. A single experimental point available in the literature [4] is also shown in this figure.

Since the energies are directly measured in the method using elastic scattering, the results here are of much better quality than those based on the Doppler shift. With a typical beam current (1–2 pnA), about 1–2 h of data collection can give better results than those with the Doppler shift method, where normally 4–6 h of measurement are necessary for each experimental point. The data for this second method were taken in two different measurements, labeled I and II in Table 2. It should be noted that this method provides a very reliable way to measure the angular distribution of the secondary beam, after traversing the stopper foil, by measuring the yield of recoiling ions as a function of the recoiling angle. These measurements may

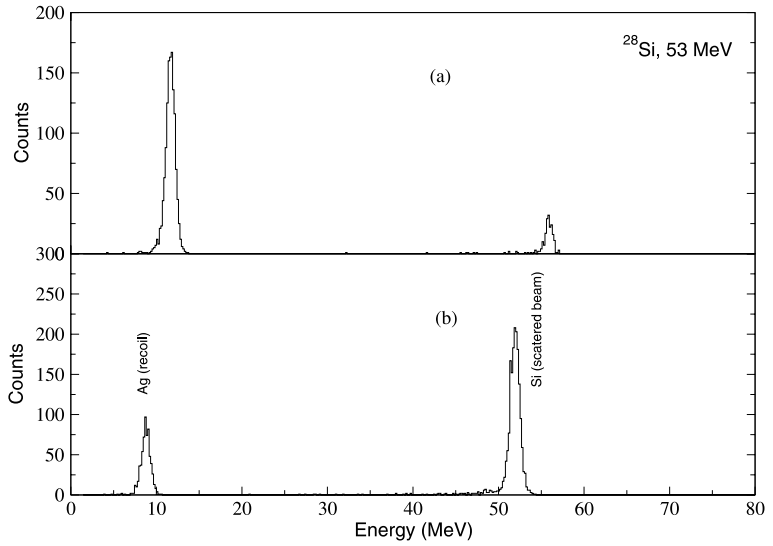


Fig. 4. Typical spectra for the energy of the particles in the recoil detector with out (a) and with (b) the stopper foil. Since the recoil and scattering angles are close, due to angular straggling the scattering peak is also seen in the recoil detector (see text).

Table 2
Stopping power of Au for Ag ions: results from the experiment using the elastic scattering method

| $E_i$ | Exp. | $\overline{E}$ | $v/v_0$ | $(dE/dx)_{exp}$ | $(dE/dx)_{fit}^{DS}$ [a] | $(dE/dx)_{ZBL}$ [b] |
|---|---|---|---|---|---|---|
| 8.4 | I | 7.20 | 1.64 | 3.10 (12) | 2.95 | 3.15 |
| 10.3 | II | 9.14 | 1.85 | 3.67 (15) | 3.54 | 3.77 |
| 11.8 | I | 10.3 | 1.96 | 4.05 (16) | 3.92 | 4.14 |
| 11.9 | II | 10.6 | 1.99 | 4.07 (16) | 4.01 | 4.26 |
| 13.3 | II | 11.9 | 2.11 | 4.40 (18) | 4.45 | 4.67 |
| 13.9 | I | 12.2 | 2.13 | 4.52 (18) | 4.54 | 4.76 |
| 15.9 | I | 14.0 | 2.29 | 5.11 (20) | 5.12 | 5.29 |

All energies are in MeV and stopping powers in MeV cm$^2$/mg. The $v/v_0$ corresponding to $\overline{E}$ is also shown. The two series of data are labeled Exp. I and Exp. II. The stopper foil used for both series was 0.62 mg/cm$^2$ thick. Most of the uncertainty in the experimental stopping power comes from the stopper thickness.

[a] Using the ZBL program [3] but with the fitted coefficients obtained from the Doppler shift data.

[b] From [3].

give important information about the process of multiple elastic scattering, for which almost no experimental data are available in the literature. Measurements of this angular distribution are in progress and will be reported later.

## 3. Discussion and conclusions

In this work, we present new data for the stopping power of gold for silver ions for energies in the range 7–50 MeV corresponding to velocities between about $1.6v_0$ and $4.4v_0$, where $v_0$ is the Bohr velocity. The data were taken using two different techniques, and excellent agreement between the two data sets was found, in the sense that the parameterized curve obtained for the data set at higher velocity, reproduces quite well the data at lower velocity (see Fig. 2). In the velocity region of the present measurements, the mechanisms of energy loss are expected to depend on the details of the electronic density in the periphery of the atom at the crystalline site. This causes an oscillatory dependence of the electronic stopping

cross section on the atomic number of the stopper element, making it difficult to extrapolate the data from other media. Thus, failure of the semiempirical formulation is not unusual in this velocity region. This can be observed when comparing experimental data with the predictions from [3]. These calculations are one of the most used and include the oscillatory aspect mentioned above. The trends observed for the present measurements (see Fig. 2) can be compared with those for other measurements in the same velocity region. In [9], for example, the data for light ions in several stopper elements show similar results to those of the present work. There is good agreement with the ZBL predictions at lower velocities, the experimental points deviating towards higher values as energy increases. In other measurements, such as the data for Nd in Pb from [10], show stopping power values larger than the ZBL predictions for all measured velocities. On the contrary, the Si in Al data from [11], and Ag in Gd [6], experimental data are below the ZBL predictions. These examples illustrate the difficulties for prediction of the stopping powers in this velocity region. A much more extensive experimental data base is necessary in order to construct more reliable semiempirical predictions for the low velocity region.

The technique based on the elastic scattering has shown to produce better results than those based on the Doppler shift, and also uses less measurement time. A second and important aspect related to this new technique is that it makes possible the measurement of the angular distribution of the recoils after passing through the stopper foil, allowing the study of the multiple elastic scattering mechanism.

## Acknowledgements

R.V.R., N.H.M., N.A., J.R.B.O. and M.N.R. would like to acknowledge financial support received from the Conselho Nacional de Desenvolvimento Científico e Tecnológico (CNPq).

## References

[1] T.K. Alexander, J.S. Forster, in: M. Baranger, E. Vogt (Eds.), Advances in Nuclear Physics, Vol. 10, Plenum Press, New York, 1978, p. 197.
[2] J.F. Ziegler, J.P. Biersack, U. Littmark, in: J.F. Ziegler (Ed.), The Stopping and Ranges of Ions in Matter, Vol. 1, Pergamon Press, Oxford, 1985.
[3] J.F. Ziegler and J.P. Biersack, SRIM2000, Available from <www.srim.org>.
[4] R.V. Ribas, W.A. Seale, W.M. Roney, E.M. Szanto, Phys. Rev. A 21 (1980) 1173.
[5] R.V. Ribas, W.A. Seale, M.N. Rao, Phys. Rev. A 28 (1983) 3234.
[6] R.V. Ribas, N.H. Medina, M.N. Rao, E.W. Cybulska, W.A. Seale, Phys. Rev. A 51 (1995) 2634.
[7] W.M. Roney, W.A. Seale, Nucl. Instr. and Meth. 138 (1976) 507.
[8] W.M. Currie, Nucl. Instr. and Meth. 73 (1969) 173.
[9] L. Xiting, X. Zonghuang, Z. Tao, S. Yixiong, Nucl. Instr. and Meth. B 168 (2000) 287.
[10] F. Brandolini, N.H. Medina, M. De Poli, P. Pavan, M. Wilheim, A. Dewald, G. Pascovici, Nucl. Instr. and Meth. B 132 (1997) 11.
[11] K. Arstila, Nucl. Instr. and Meth. B 168 (2000) 473.